Desalination and Water Treatment
www.deswater.com

doi: 10.1080/19443994.2014.996775

57 (2016) 4898–4905
March

Taylor & Francis
Taylor & Francis Group

Near-field dilution of a vertical dense jet impinging on a solid boundary

G.C. Christodoulou*, I.K. Nikiforakis, T.D. Diamantis, A.I. Stamou

Applied Hydraulics Laboratory, School of Civil Engineering, National Technical University of Athens, 5 Heroon Polytechniou St., Zografou 15780, Greece, Tel. +30 2107722813; Fax: +30 2107722814; email: christod@hydro.ntua.gr (G.C. Christodoulou), Tel. +30 2107722801; Fax: +30 2107722814; email: giannisnikiforakis@gmail.com (I.K. Nikiforakis), Tel. +30 2103477436; email: thomas.di.diamantis@gmail.com (T.D. Diamantis), Tel. +30 2107722809; Fax: +30 2107722814; email: stamou@central.ntua.gr (A.I. Stamou)

Received 18 June 2014; Accepted 2 December 2014

ABSTRACT

Experimental measurements of concentrations were performed for vertical dense jets discharged downwards to a horizontal or a sloping bottom, aiming at: (a) determining the dilution at the impingement point on a solid bed and assess the influence of the boundary, and (b) evaluating the additional dilution achieved within the density current, which forms in the vicinity of the impingement point. It is found that the presence of the solid boundary affects the axial dilution of the approaching jet up to a distance of h_D, which is well correlated to the source height and the length scale L_M. The dilution at the impingement point on the boundary is reduced appreciably compared to that of a boundary-free jet at the same location. The additional dilution within the density current on a sloping bottom is well correlated to the dimensionless distance from the impingement point. Dimensionless empirical equations are proposed for the dilution at the impingement point and in the density current near the bed, in terms of geometrical parameters and the densimetric Froude number.

Keywords: Desalination; Dense jets; Brine disposal; Marine outfalls; Dilution

1. Introduction

Brine effluents from land-based and offshore desalination plants are commonly discharged into coastal waters through either submerged outfalls or as surface discharges. In most cases, the effluents are heavier than ambient, notably those from reverse osmosis plants, which are predominant worldwide. Irrespective of the initial discharge orientation, the resulting dense jets eventually impinge on the sea bed and spread as density currents. The increased salt concentration of the brine, as well as the contained traces of chemicals from the desalination process, may thus cause negative effects on the benthic flora and fauna. From a practical point of view, the dilutions achieved at the impact point and its vicinity are most important, as they imply the highest concentrations on the floor of any harmful substances contained in the effluent.

Dense brine effluents from submerged outfalls are usually discharged inclined upwards, as negatively buoyant jets (NBJ), to increase their trajectory and dilution. Upon reaching the terminal rise height, the flow reverses and falls toward the bottom, becoming positively buoyant jets (PBJ). Effluents from offshore desalination plants are normally discharged downwards as PBJ. In both cases, after jet impingement on

*Corresponding author.

the boundary, a density current forms and spreads on the bottom. Although, in the literature, many works can be found concerning the development of PBJ, e.g. [1–3]; and NBJ, e.g. [4–9]; the study of the effect of boundary proximity has received little attention. Recently, Ramakanth et al. [10] found that in the presence of a solid boundary the dilution at the return point of NBJ, namely at the point where the jet returns to the source elevation, is reduced compared to the respective boundary-free flow. Cavalletti and Davies [11] observed that the velocity fields of plane vertical dense jets are disturbed as the jet approaches a rigid boundary. Concerning the characteristics of the density current, the spreading of its visual boundary was studied recently, e.g. [12], but few concentration/dilution measurements have been reported so far [4,13–15].

The objective of this paper is to (a) determine the dilution at impingement of dense jets on a solid bed and assess the influence of the boundary, and (b) evaluate the additional dilution achieved within the density current in the vicinity of the impingement point. To this end, experimental results for vertical dense jets are presented, derived from two series of experiments, as described below. The vertical jet case was selected, because the axis and the impingement point are known a priori, thus facilitating the experiments, and also as a necessary first step to the study of oblique impingement as in the case of NBJ.

2. Experiments

The reported results were obtained from two series of experiments:

(1) Vertical dense jets discharged downwards on a horizontal bottom, in which concentrations were measured within the jet at certain distances from the boundary.

(2) Vertical dense jets discharged downwards on a 5° sloping bottom, in which concentrations were measured at selected locations within the density current.

All experiments were conducted in the Applied Hydraulics Laboratory of the National Technical University of Athens, in a tank of 3.0 m long, 1.5 m wide, and 0.9 m deep, shown in Fig. 1, whereas a notation sketch is given in Fig. 2. In Series (1), a false horizontal ($\varphi = 0^o$) bottom with dimensions 1.05 m × 0.50 m (length × width) was introduced at a distance of 18 cm above the tank bottom. In Series (2), a plexiglass bottom slab was introduced at an angle of $\varphi = 5^o$ to the horizontal. Round pipes of diameter $D = 0.8$, 1.0, and 1.6 cm, were used to discharge the jet vertically downwards. In Series (2), the distance between the discharge point and the inclined bottom was constant, approximately $H = 48$ cm, whereas in Series (1) the distance was variable. The tank was initially filled up with tap water, and the jet effluent was salt water solution colored with blue dye of density 1.9–5.5% higher than the ambient. The densities of the salt water solution (ρ_o) and the tank water ($\rho_a < \rho_o$) were calculated from their salinity (ppt) and temperature (°C) values measured by a portable instrument (YSI Model 30). These densities were generally in good agreement with the densities measured by a hydrometer and by weighting, using KERN scale EMB 2200-0, a known volume of sample contained in a calibrated flask. The flow rate of the salt water effluent was measured by means of a Venturi meter combined with a differential manometer and a volumetric cylinder. Concentration measurements concerning salinity were performed by using a microscale conductivity and temperature instrument manufactured by Precision Measurement Engineering, USA (Model 125).

Basic parameters which are known [4] to govern the behavior of buoyant jets are the initial (at the

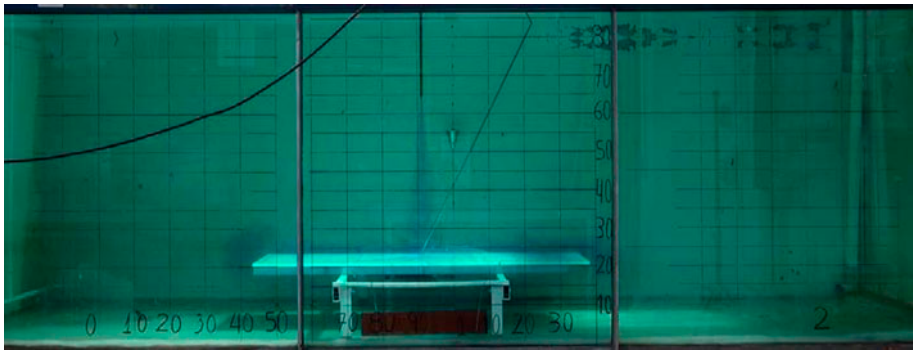

Fig. 1. Experimental tank; typical experiment of Series 1.

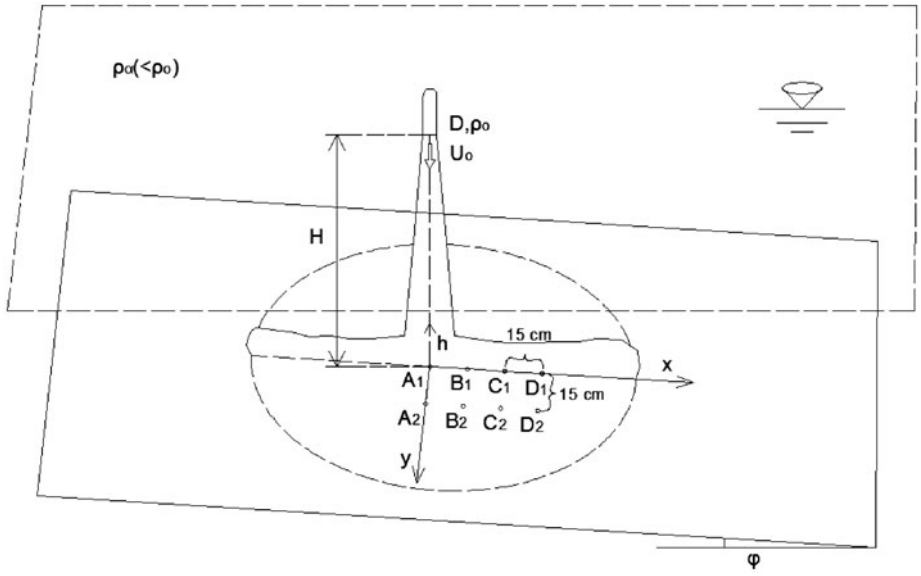

Fig. 2. Notation sketch showing the visual boundary of the density current and the measurement points on the bottom in Series 2; A1 is the impingement point.

source) densimetric Froude number, F_o and the momentum-to-buoyancy length scale, L_M, defined as:

$$F_o = \frac{U_o}{\sqrt{g_o' D}} = \frac{Q_o}{\pi \sqrt{g_o' D^5}} \quad (1a)$$

$$L_M = \frac{M_o^{3/4}}{B_o^{1/2}} = \left(\frac{\pi}{4}\right)^{1/4} D F_o \quad (1b)$$

where U_o is the exit flow velocity, g_o' is the apparent gravitational acceleration, which is equal to $g|\rho_a - \rho_o|/\rho_a$ and Q_o, M_o, and B_o are the initial kinematic fluxes of volume, momentum, and buoyancy, respectively.

In the present experiments, the initial densimetric Froude numbers F_o were approximately 3.5, 11, 17, and 23, chosen so as to identify possible differences due to high/low values of F_o. In all cases, the Reynolds number was sufficiently high in the range 2,997–6,954, thus, the jets were always turbulent. Table 1 summarizes the main experimental parameters. The measurement points in the density current in Series (2) were located at 15 cm distances along the x axis (positive downslope) and on a line parallel to it at a lateral distance y = 15 cm (see Fig. 2), and at vertical distances of 1, 2, 3, 4, 5, and 6 cm from the bottom. In Series (1), measurements were taken on the jet axis at distances h = 1, 2, 3, 4, 5, 6, 7, 10, 15, and 22 cm from the horizontal solid boundary. The duration of measurements at each point was approximately 30 s to

Table 1
Summary of experimental conditions

Series	Number of runs	F_o –	D cm	Q_o cm^3/s	H cm	L_M cm	H/L_M –
Series 1							
Exp.1	1	≈3.5	1.6	38.05	43.1	5.28	8.16
Exp.2	1	≈11.0	1.0	38.37	34.6	10.57	3.27
Exp.3	1	≈17.0	0.8	32.89	47.9	12.83	3.73
Exp.4	1	≈23.0	0.8	44.13	47.9	17.11	2.80
Series 2							
Exps.5–12	8	≈3.5	1.6	53.78–59.20	48.0	5.06–5.67	8.46–9.49
Exps.12–18	7	≈17.0	0.8	44.56–55.81	48.0	12.46–13.69	3.51–3.85
Exps.19–26	8	≈23.0	0.8	49.18–59.82	48.0	17.22–17.72	2.71–2.79

allow reliable calculation of the mean (time-average) concentration due to the highly turbulent character of the flow.

Based on point concentration measurements (C), dilutions (S) from source are calculated using Eq. (2).

$$S = (C_o - C_a)/(C - C_a) \quad (2)$$

where C_a is the ambient concentration, and C_o is the source concentration. Therefore, the dilutions on the jet axis (S_c), impingement point (S_{imp}), and in the density current on the inclined bottom (S_m) can be derived by introducing the respective measured concentrations C_c, C_{imp}, and C_m in Eq. (2).

3. Results

3.1. Dilution at impingement point and effect of boundary

In Series 1, concentrations (and hence dilutions) were measured on the axis of the vertical jet at several distances from the horizontal boundary. The results are plotted in non-dimensional form, following [1,16], in Fig. 3 for initial Froude numbers $F_o \approx 3.5$ and 17, where h is the distance from the boundary (see Fig. 2). Similar plots were obtained for the other two values of F_o. Since the vertical dense jets are positively buoyant, Fig. 3 also shows the respective values calculated according to the general equation proposed by List and Imberger [17], which (for a distance h above the boundary) is:

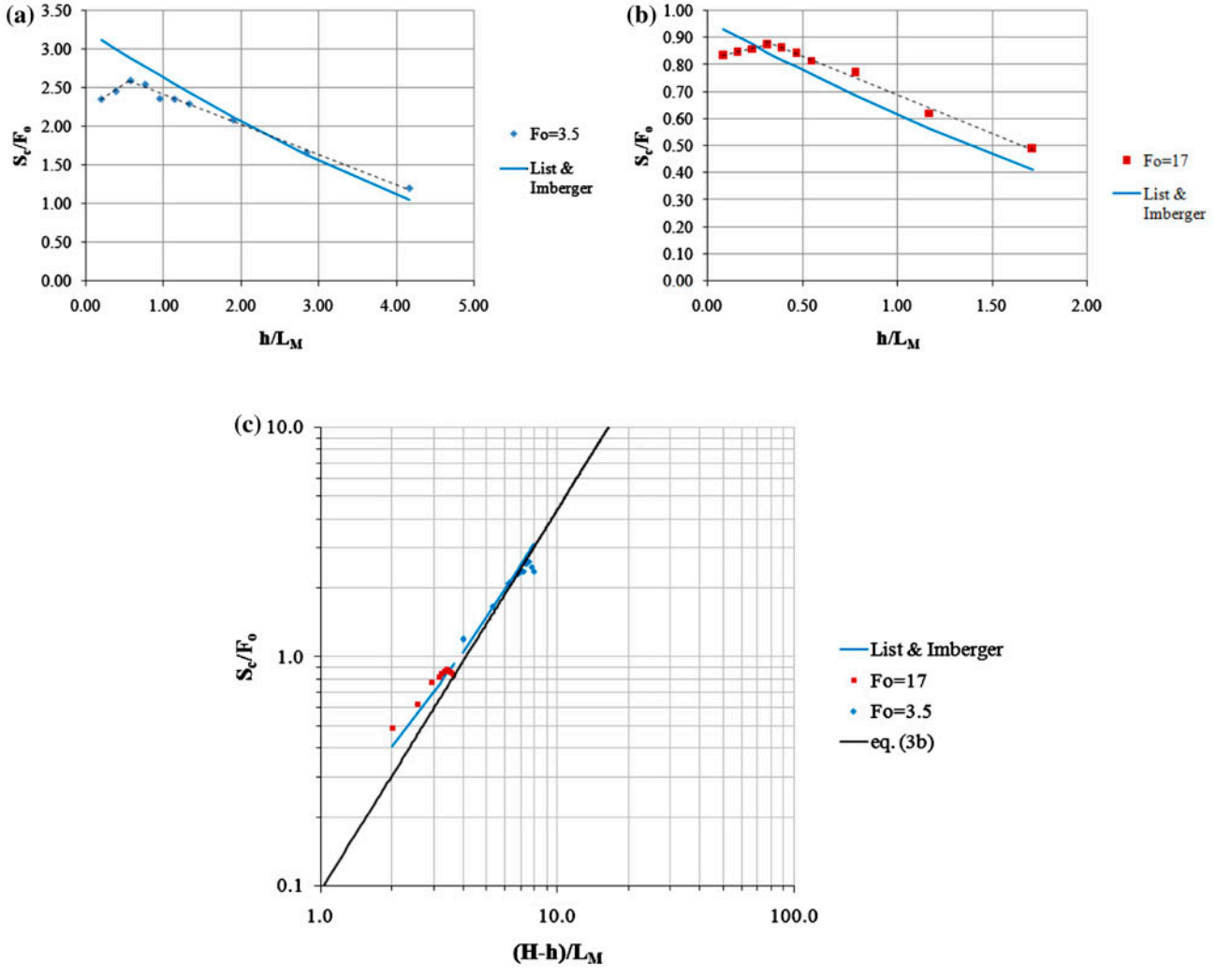

Fig. 3. Measured axial concentration and theoretical solution (Eq. (3a)) of vertical jet (a) for $F_o \approx 3.5$, (b) for $F_o \approx 17$, and (c) comparison of the results with the asymptotic plume solution (Eq. (3b)).

$$S_{ave} = \left(\frac{H-h}{z_o}\right)\left\{1+\left(\frac{R_o}{R_p}\right)^2\left[\left(\frac{H-h}{z_o}\right)^2-1\right]\right\}^{1/3} \quad (3a)$$

where R_o is the initial Richardson number, which is equal to $(1/F_o)(\pi/4)^{1/4}$, $R_p = 0.63$ is the Richardson number for the pure plume, and $z_o = 3.28D$.

For a pure plume, i.e. $R_o = R_p$, the asymptotic solution is derived as:

$$S_{ave} = \left(\frac{H-h}{z_o}\right)^{5/3} \quad (3b)$$

The calculated average cross-sectional dilutions (S_{ave}) by Eq. (3) are divided by the factor 1.7 to obtain minimum axial dilutions S_c according to [16], so as to be compatible with the measured ones. The validity of Eq. (3) for a free, positively buoyant, jet was checked prior to its implementation by comparing experimental measurements [1,18] and the Corjet model [16].

As evident in Fig. 3(a) and (b), the measured values decrease with distance from the boundary following reasonably well the theoretical prediction for a free jet, however a clear change of rate, even reversal in the evolution of S_c occurs near the solid boundary. This implies that close to the boundary the dilution is definitely less than it would be for a boundary-free jet, and may be even less than the dilution in the jet at some small distance from the bed. This effect is probably due primarily to the inability of the jet to entrain ambient fluid in the vicinity of the boundary [3]. In addition, the deflection of the jet due to the boundary and the consequent flow curvature may cause some sorting of the higher concentration fluid towards the jet axis. The extent of influence of the boundary can be quantified by means of the distance h_D, where the change of dilution behavior is observed. By fitting straight lines to the measured values close and away from the boundary as shown in Fig. 3(a) and (b), h_D is determined and given in dimensionless terms in Table 2. The observed distances of influence are smaller than those derived for a two-dimensional buoyant jet by Cavaletti and Davies [11], who proposed $h_D/L_M = 0.4$ for $1 < H/L_M < 5$ and $h_D/L_M = 0.6$–0.7 for $H/L_M > 5$. This difference is reasonable considering that in the two-dimensional case the development of the jet is constricted in one direction.

Table 3 summarizes the results of dilution for distances $h = 1$ and 4 cm. It is seen that the theoretical dilution estimates (referring to free jets) are considerably larger than the measured values at a distance of 1 cm, but the difference is reduced at a distance of 4 cm. Table 3 also includes (last column) the calculated local densimetric Froude number on the jet axis at a distance of 4 cm from the boundary, derived from Eq. (4) [17]:

$$F = \left(\frac{\pi}{4}\right)^{1/4}\cdot\left\{1+\left(\frac{R_o}{R_p}\right)^2\left[\left(\frac{H-h}{z_o}\right)^2-1\right]\right\}^{1/2} \cdot\left[R_p\left(\frac{H-h}{z_o}\right)\left(\frac{R_o}{R_p}\right)\right]^{-1} \quad (4)$$

For a pure plume ($R_p = 0.63$), the respective value of F is $F_p = 1.49$.

Table 2
Height (h_D) of boundary influence in a vertical jet

	F_o –	H/L_M –	h_D cm	h_D/L_M –
Exp.1	3.5	8.16	2.96	0.56
Exp.2	11.0	3.27	3.17	0.30
Exp.3	17.0	3.73	4.23	0.33
Exp.4	23.0	2.80	4.28	0.25

Table 3
Measured and calculated dilutions in a vertical jet

				$h = 1$ cm			$h = 4$ cm			
				Measured		Calculated	Measured		Calculated	
	F_o –	C_o ppt	C_a ppt	C_{imp} ppt	S_c –	S_c –	C_{imp} ppt	S_c –	S_c –	F
Exp.1	3.5	27.6	0.2	3.51	8.28	10.96	3.26	8.95	9.72	1.55
Exp.2	11.0	28.0	0.2	4.27	6.83	8.53	4.48	6.50	7.48	1.91
Exp.3	17.0	27.7	0.2	2.13	14.25	15.89	2.04	14.95	14.42	1.81
Exp.4	23.0	27.5	0.2	2.23	13.45	14.04	2.37	12.56	12.82	2.02

A non-dimensional plot showing the effect of the boundary is given in Fig. 4.

The non-dimensional distance h_D/L_M is well linearly correlated to the non-dimensional source elevation H/L_M, as follows:

$$h_D/L_M = 0.054\ (H/L_M) + 0.118 \quad (5)$$

Further, the measured dilutions at $h = 1$ cm, normalized by F_o, are well correlated with the respective distance from the source, normalized with the length scale L_M, as depicted in Fig. 5 and expressed by Eq. (6), in which both h and L_M are expressed in cm. This correlation allows the approximate estimate of the impingement dilutions in the experiments of Series 2, where they were not measured directly.

$$S_{imp}/F_o = 0.349\ (H - 1.0)/L_M - 0.434 \quad (6)$$

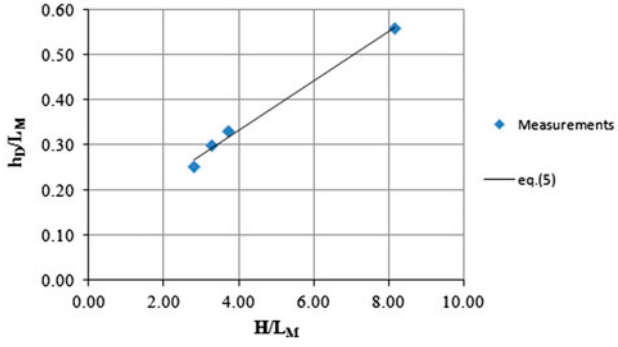

Fig. 4. Variation of dimensionless distance h_D/L_M with source elevation H/L_M.

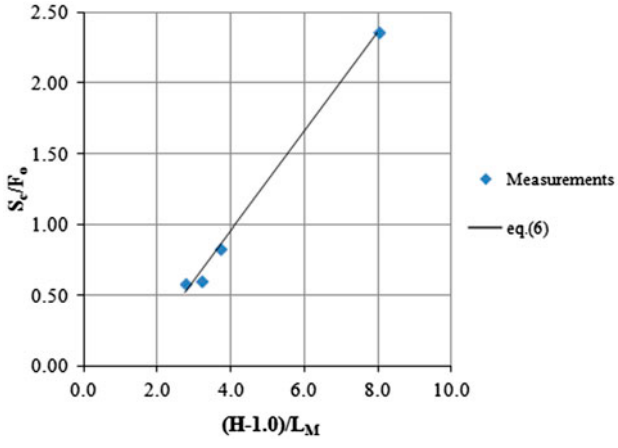

Fig. 5. Variation of normalized measured dilution at the impingement point at 1 cm above the boundary, with the normalized distance from the source.

3.2. Additional dilution in density current

According to measurements in previous studies [4,13,14], the vertical concentration profiles within the density current are approximately linear; therefore, the highest concentrations are near the bed. Fig. 6 presents the additional near-bed (i.e. at the closest measurable distance of 1 cm) dilution (S_L) relative to the impingement point vs. the respective distance L_i for the experiments of Series 2. The dilution values were calculated according to Eq. (2) from the measured total dilutions S_m, and the respective impingement dilutions S_{imp} obtained from the correlation of Eq. (6), as $S_L = S_m/S_{imp}$. An apparently linear correlation is observed for each Froude number within our experimental range, given the usually large scatter present in this type of measurements (e.g. [4]). It may be further noted that previous experiments by Roberts et al. [4] in a narrower tank concerning dilution within the density current following the impingement of a dense jet on a horizontal bottom, suggested that the dilution becomes nearly constant at a normalized distance L_i/DF_o about 7, defined as the "end of mixing zone." The present data points seem to be mostly below that limit, although there is some evidence in the case of $F_o = 3.5$ that the dilution may indeed tend to become constant as L_i/DF_o increases near the specified value.

Fig. 7 presents the same results, but normalizing both S_L and the distance L_i by the Froude number F of the jet, given by Eq. (4), at $h = 4$ cm, where, in the present experiments, the interference of the solid boundary approximately starts. One may notice that the results for "large" initial Froude numbers (i.e. 17 and 23) almost coincide, whereas they are distinctly different for the "small" initial Froude number (i.e. 3.5). This can be explained by looking at the values of H/L_M in this group of experiments (see Table 1). It is

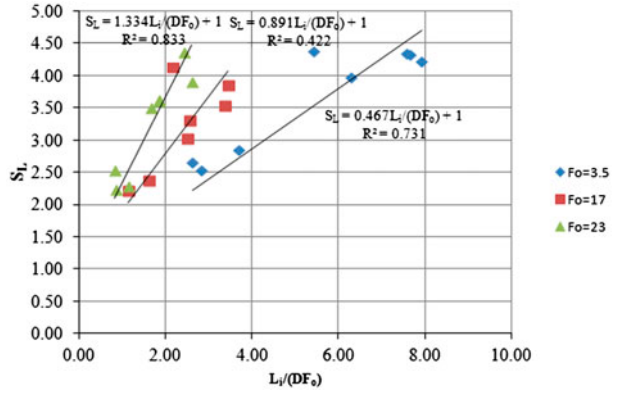

Fig. 6. Variation of additional near-bed (at 1 cm) dilution S_L with normalized distance from the impingement point.

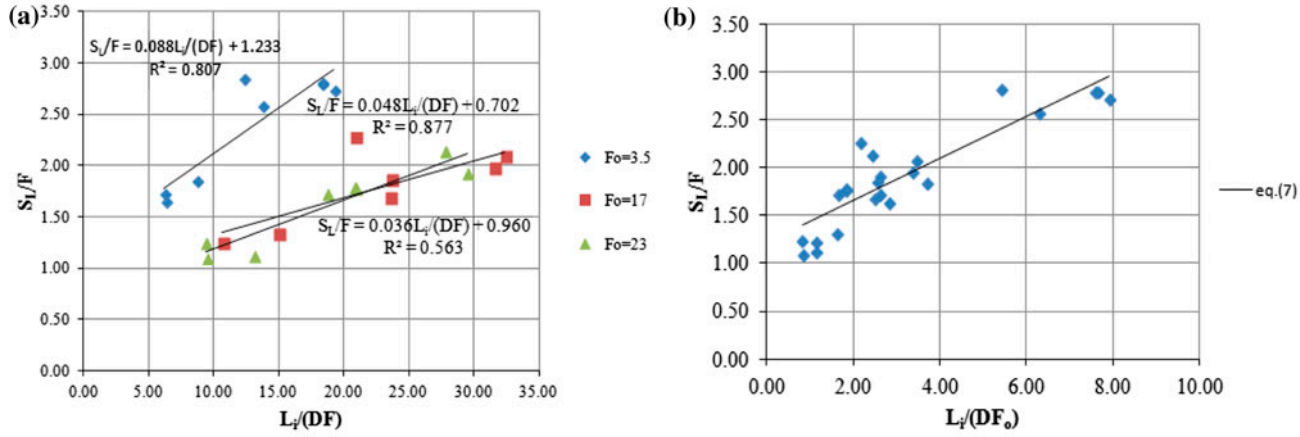

Fig. 7. Normalized additional dilution near the bed vs. (a) distance L_i normalized with F at $h = 4$ cm, and (b) distance L_i normalized with F_o.

seen that for the initial $F_o \approx 3.5$ the value of $H/L_M > 8.46 > 5$, whereas for the other two F_o, it is $H/L_M < 5$. This implies, according to Papanicolaou and List [1] that the dense jet has become a plume prior to impingement in the first case, but not in the other two. Also, according to Table 3, in the case of $F_o \approx 3.5$ the local value of F at $h = 4$ cm is 1.55, very close to the pure plume value 1.49. The plume character of flow of the $F_o \approx 3.5$ jet before its impingement is further verified by its approach to the asymptotic plume solution depicted in Fig. 3(c). Still, if the distance L_i is normalized by F_o the behavior of S_L/F is the same for all experiments (Fig. 7(b)) described by Eq. (7):

$$S_L/F = 0.220 \cdot L_i/(DF_o) + 1.214 \quad (7)$$

Finally, Fig. 8 shows the total dilution S_m on the floor normalized by F_o vs. the non-dimensional vertical distance H/L_M from the source. Despite considerable scatter, an overall linear trend is observed, expressed by Eq. (8). A linear correlation between S_m/F_o and H/L_M was also proposed by Abessi et al. [15] for dense surface discharges impinging on a horizontal bottom.

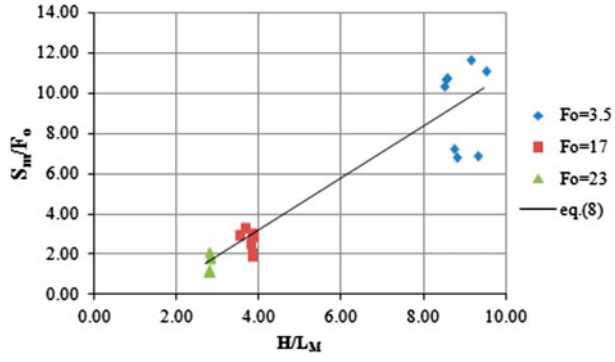

Fig. 8. Normalized total dilution on the bottom vs. source height.

$$S_m/F_o = 1.285 \cdot H/L_M - 1.961 \quad (8)$$

4. Conclusions

Experimental measurements of concentrations were performed for round vertical dense jets discharged downwards to a horizontal or a sloping bottom. The main conclusions are summarized as follows:

(1) The presence of the solid boundary affects the axial dilution of the approaching jet up to a distance of h_D, which is well correlated to the source height and the length scale L_M.
(2) The dilution at the impingement point on the boundary is reduced appreciably compared to that of a boundary-free jet at the same location.
(3) The additional dilution achieved within the density current which spreads on a sloping bottom is well correlated to the dimensionless distance from the impingement point.
(4) Empirical equations are derived for expressing the normalized additional near-bed dilution in terms of the dimensionless distance from the impingement point as well as the total dilution in terms of the dimensionless source height.

The proposed dimensionless equations may be useful for estimating the dilutions and concentrations

in the vicinity of the impingement point of vertical dense jets discharged downwards as PBJ associated with brine disposal from offshore desalination plants. They may also give approximate estimates of the near-bed dilution of inclined dense jets discharged from submerged brine outfalls as NBJ, which often impinge on the bottom at an angle close to vertical. Nevertheless, further work is needed to explore the degree of validity of the results for NBJ.

Acknowledgments

Research leading to this paper was partly co-financed by the European Union (European Social Fund—ESF) and Greek national funds through the Operational Program "Education and Lifelong Learning" of the National Strategic Reference Framework (NSRF)—Research Funding Program: Heracleitus II. Investing in knowledge society through the European Social Fund.

Notation

B_o — initial kinematic buoyancy flux
C_o — source concentration
C_a — ambient concentration
C_c — jet axial concentration
C_m — local measured concentration
C_{imp} — concentration at the jet impingement point
D — jet source diameter
F_o — initial densimetric Froude number of the jet
F — local densimetric Froude number of the jet
g_o' — initial apparent gravitational acceleration
h — distance above the boundary (bottom)
H — height of source above the bottom
h_D — height of boundary influence in a vertical jet
L_i — distance between a concentration measurement point and the jet impingement point
L_M — momentum-to-buoyancy length scale
M_o — initial kinematic momentum flux
Q_o — initial kinematic volume flux
R_o — initial Richardson number
R_p — Richardson number for the pure plume
S_c — jet axial dilution
S_{imp} — impingement dilution
S_m — total dilution (relative to the source)
S_L — additional dilution (relative to the impingement point)
S_{ave} — calculated average cross-sectional dilution of the jet
U_o — jet exit velocity
z_o — equal to $3.28D$

References

[1] P. Papanicolaou, J. List, Investigations of round vertical turbulent buoyant jets, J. Fluid Mech. 195 (1988) 341–391.
[2] G. Noutsopoulos, P. Yannopoulos, The round vertical turbulent buoyant jet, J. Hydraul. Res. 25(4) (1987) 481–502.
[3] J.H.W. Lee, G.H. Jirka, Vertical round buoyant jet in shallow water, J. Hydraul. Div. ASCE 107 (1981) 1651–1675.
[4] P.J.W. Roberts, A. Ferrier, G. Daviero, Mixing of inclined dense jets, J. Hydraul. Eng. ASCE 123(8) (1997) 693–699.
[5] I.G. Papakonstantis, G.C. Christodoulou, P.N. Papanicolaou, Inclined negatively buoyant jets 1: Geometrical characteristics, J. Hydraul. Res. 49(1) (2011a) 3–12.
[6] I.G. Papakonstantis, G.C. Christodoulou, P.N. Papanicolaou, Inclined negatively buoyant jets 2: Concentration measurements, J. Hydraul. Res. 49(1) (2011b) 13–22.
[7] G.A. Kikkert, M.J. Davidson, R.I. Nokes, Inclined negatively buoyant discharges, J. Hydraul. Eng. ASCE 133 (5) (2007) 545–554.
[8] C.C.K. Lai, J.H.W. Lee, Mixing of inclined dense jets in stationary ambient, J. Hydro-Environ. Res. 6 (2012) 9–28.
[9] D. Shao, A.W.K. Law, Mixing and boundary interactions of 30° and 45° inclined dense jets, Environ. Fluid Mech. 10 (2010) 521–553.
[10] A. Ramakanth, M.J. Davidson, R. Nokes, Influence of a boundary on negatively buoyant jets, in: ISEH VII Organisers (Ed.), Proceedings of 7th International Symposium on Environmental Hydraulics, Singapore, 2014, pp. 86–89.
[11] A. Cavalletti, P.A. Davies, Impact of vertical, turbulent, planar, negatively buoyant jet with rigid horizontal bottom boundary, J. Hydraul. Eng. ASCE 129(1) (2003) 54–62.
[12] I.G. Papakonstantis, G.C. Christodoulou, Spreading of round dense jets impinging on a horizontal bottom, J. Hydro-Environ. Res. 4 (2010) 289–300.
[13] I.K. Nikiforakis, G.C. Christodoulou, A.I. Stamou, Spreading of vertical dense jets on a sloping bottom: Concentration measurements, in: T.D. Lekkas (Ed.), Proceedings of the 13th International Conference on Environmental Science and Technology, Athens, Greece, 2013.
[14] I.K. Nikiforakis, G.C. Christodoulou, A.I. Stamou, Bottom concentration field due to impingement of inclined dense jets on a slope, in: ISEH VII Organisers (Ed.), Proceedings of the 7th International Symposium on Environmental Hydraulics, Singapore, 2014, pp. 54–57.
[15] O. Abessi, M. Saeedi, T. Bleninger, M. Davidson, Surface discharge of negatively buoyant effluent in unstratified stagnant water, J. Hydro-Environ. Res. 6 (2012) 181–193.
[16] G.H. Jirka, Integral model for turbulent buoyant jets in unbounded stratified flows. Part I: The single round jet, Environ. Fluid Mech. 4 (2004) 1–56.
[17] E.J. List, J. Imberger, Turbulent entrainment in buoyant jets, J. Hydraul. Div. ASCE 99 (1973) 1461–1474.
[18] H. Wang, A.W.K. Law, Second-order integral model for a round buoyant jet, J. Fluid Mech. 459 (2002) 397–428.